

# Beyond One-Size-Fits-All: Neural Networks for Differentially Private Tabular Data Synthesis

Kai Chen, Chen Gong, Tianhao Wang  
University of Virginia

**Abstract**—In differentially private (DP) tabular data synthesis, the consensus is that statistical models are better than neural network (NN)-based methods. However, we argue that this conclusion is incomplete and overlooks the challenge of densely correlated datasets, where intricate dependencies can overwhelm statistical models. In such complex scenarios, neural networks are more suitable due to their capacity to fit complex distributions by learning directly from samples. Despite this potential, existing NN-based algorithms still suffer from significant limitations. We therefore propose MargNet, incorporating successful algorithmic designs of statistical models into neural networks. MargNet applies an adaptive marginal selection strategy and trains the neural networks to generate data that conforms to the selected marginals. On sparsely correlated datasets, our approach achieves utility close to the best statistical method while offering an average  $7\times$  speedup over it. More importantly, on densely correlated datasets, MargNet establishes a new state-of-the-art, reducing fidelity error by up to 26% compared to the previous best. We release our code on GitHub.<sup>1</sup>

## 1. Introduction

Differential privacy (DP) for tabular data generation enables researchers and practitioners to share useful synthetic datasets with a quantifiable privacy guarantee. With the increasing research and application demands for tabular data [1], [2], [3], [4], effective methods for privately generating tabular data have received much attention [5], [6], [7], [8], [9], [10], [11], [12], [13].

Existing solutions to DP tabular data synthesis are often categorized into “statistical methods”, which usually build probabilistic models from low-dimensional statistics, and “neural network-based methods”, which generate data using neural networks [11]. Among them, AIM [5], a statistical approach, has been consistently recognized as the state-of-the-art solution across existing benchmarks [10], [14]. AIM’s success stems from two key aspects: adaptive selection of informative marginals (statistical distributions over attribute subsets) and efficient joint distribution modeling through the private-probabilistic graphical model (PGM). The adaptive marginal selection prioritizes the capture of the most informative local distributions with a limited privacy budget.

While PGM can construct a chain-like sequence of attribute cliques with a subset of marginals, and model the joint distribution by only estimating those cliques’ distributions and applying the chain rule of probability to them.

The superiority of AIM has been analyzed and discussed in various previous studies [5], [10], [11]. Nevertheless, the main drawback of this approach is overlooked by them: its limitation in dealing with complex correlations between attributes. For example, if we use AIM to synthesize a dataset where each attribute shows strong correlations with many other attributes, a large number of marginals are needed to capture those correlations. These marginals, together building a dense graph, cause the clique domain size to grow exponentially and become computationally prohibitive. This leads to two consequences. First, the time efficiency of AIM decreases sharply due to the estimation of clique distributions with large domain sizes. Second, when the domain sizes of cliques reach a threshold, AIM is forced to discard certain correlations, even highly informative, and estimate them with the conditional independence assumption between cliques, which may not be valid in these scenarios and thus causes utility degradation.

Regarding these limitations, neural networks appear as a natural alternative, due to their phenomenal black-box data distribution fitting capability by directly generating samples. Various neural network-based methods have been proposed to contribute to DP tabular data synthesis. For instance, several approaches [11], [15], [16], [17], [18], [19], [20] apply the DP Stochastic Gradient Descent (DP-SGD) technique to train neural networks, such as Generative Adversarial Networks (GANs), diffusion models, and Large Language Models (LLMs). Additionally, some methods incorporate statistical features into model training. For instance, PATE-GAN [21] privatizes a voting statistical histogram from multiple teacher discriminators. The histogram aims to train a student discriminator that guides the generator training. Moreover, DP-MERF [13] and GEM [12] use random Fourier features and marginal queries to construct loss functions and train neural networks, respectively.

However, even though numerous efforts have been devoted to neural network-based approaches, their expected superiority has not been validated by any previous study: AIM consistently demonstrates superior generation utility over these methods. We attribute this discrepancy to the limitations in prior works. (1) *Imperfect Algorithm Design*. The algorithmic designs of existing NN-based methods fail

1. <https://github.com/KaiChen9909/margnet>

to fully leverage the potential of neural networks. On the one hand, several empirical studies [10], [11] have proven that DP-SGD is inefficient at capturing tabular data distributions, especially under a limited privacy budget. On the other hand, for those NN-based methods on statistical features, the effectiveness of these features is often insufficient, leading to suboptimal utility in prior empirical studies [10], [11]. (2) *Incomplete Evaluation*. Another limitation is that existing evaluations cannot fully validate the potential of neural networks. Previous evaluations [5], [10], [11], [12], [13], [22] are often conducted on datasets that are highly homogeneous and only contain sparse correlations between variables. Consequently, these assessments are confined to a superficial level, overlooking more challenging scenarios, such as data with densely correlated attributes. This latter scenario, as we discussed, is precisely the domain where neural networks can hold a significant advantage.

These limitations prevent us from verifying whether neural networks are a feasible alternative to the widely recognized state-of-the-art method, AIM, especially on complex datasets. Therefore, we propose this work. Our contributions can be summarized as follows.

- **New Method.** Recognizing the limitations of AIM in generating complex datasets (e.g., densely correlated datasets), we propose a new algorithm as an alternative for these scenarios. Specifically, to leverage the capacity of neural networks in fitting complex correlations, we introduce MargNet. It applies an adaptive marginal selection strategy to capture distribution information and fits marginals with neural networks. We also provide a theoretical evaluation of its fitting error.
- **Extensive Experimental Validation.** To provide a more comprehensive validation than previous empirical studies [10], [11], we conduct our evaluation around two distinct categories of datasets: sparsely correlated datasets and densely correlated datasets. On the sparsely correlated datasets, we verify that MargNet outperforms existing neural network-based methods in generative utility. On these datasets, while MargNet’s utility lags behind AIM in some cases (e.g., low privacy budget), it offers better time efficiency, achieving an average  $7\times$  acceleration over AIM. More importantly, on densely correlated datasets, MargNet leverages its ability to effectively fit densely distributed marginals and achieve superior synthesis utility, reducing the fidelity error by up to 26% compared to the previously state-of-the-art algorithm.
- **Insights for Algorithm Selection.** Beyond past studies, this work challenges the historically held view that PGM-based statistical methods are the universal state-of-the-art solution in synthesis utility [5], [10], [11]. The success of MargNet guides us to rethink an important research question of how to select the most appropriate generative algorithm based on the characteristics of a given dataset. In our experiments, we prove that the effectiveness of graph-based statistical synthesis methods, like AIM, is highly dependent on the characteristics of the dataset. In many scenarios, PGM’s powerful ability to fit measured

marginals and infer unmeasured correlations can indeed yield excellent generative performance. However, in more complex situations, such as on the densely correlated datasets in our experiments, this approach can lose its effectiveness. These observations offer deeper insights into the DP tabular data synthesis problem.

## 2. Preliminaries

### 2.1. DP Definition

Differential privacy (DP) enables the extraction of aggregated statistical information while limiting the disclosure of information about individual users. Formally, the definition of DP is given by:

**Definition 1** (Differential Privacy). An algorithm  $\mathcal{A}$  satisfies  $(\epsilon, \delta)$ -differential privacy (DP) if and only if for any two neighboring datasets  $D$  and  $D'$  and any  $T \subseteq \text{Range}(\mathbf{A})$ ,

$$\Pr[\mathcal{A}(D) \in T] \leq e^\epsilon \Pr[\mathcal{A}(D') \in T] + \delta.$$

Here, we say two datasets are neighboring ( $D \simeq D'$ ) when they only differ on one tuple/sample (via adding or removing one sample). In practice, instead of using DP, researchers often use zero-Concentrated DP (zCDP) [23] as a tight composition tool [5], [6], [9], which is important in designing complex algorithms composed of multiple modules that satisfy DP. We give the definition of zCDP and its properties as follows.

**Definition 2** (zero-Concentrated DP [23]). An algorithm  $\mathcal{A}$  satisfies  $\rho$ -zCDP if and only if for any two neighboring datasets  $D$  and  $D'$  and  $\alpha > 1$ ,  $D_\alpha(\mathcal{A}(D) || \mathcal{A}(D')) \leq \rho \cdot \alpha$ , where  $D_\alpha(P || Q) = \frac{1}{\alpha-1} \ln \mathbb{E}_{x \sim Q} \left[ \frac{P(x)}{Q(x)} \right]^\alpha$ .

zCDP has composition and post-processing properties [23], which makes it a suitable choice for complex algorithm design.

**Proposition 1** (Composition). Let  $f : \mathcal{D} \rightarrow \mathcal{R}_1$  be  $\rho_1$ -zCDP and  $g : \mathcal{R}_1 \times \mathcal{D} \rightarrow \mathcal{R}_2$  be  $\rho_2$ -zCDP respectively. Then the mechanism defined as  $(X, Y)$ , where  $X \sim f(D)$  and  $Y \sim g(D, f(D))$ , satisfies  $(\rho_1 + \rho_2)$ -zCDP.

**Proposition 2** (Post-Processing). Let  $f : \mathcal{D} \rightarrow \mathcal{R}_1$  is  $\rho$ -zCDP, and  $g : \mathcal{R}_1 \rightarrow \mathcal{R}_2$  is an arbitrary randomized mapping. Then  $g \circ f$  is also  $\rho$ -zCDP.

Moreover, a  $\rho$ -zCDP guarantee can easily be converted to a  $(\epsilon, \delta)$ -DP guarantee via Proposition 3 [23].

**Proposition 3.** If  $f$  is an  $\rho$ -zCDP mechanism, then it also satisfies  $(\epsilon, \delta)$ -DP for  $\forall \epsilon > 0$  and,

$$\delta = \min_{\alpha > 1} \frac{\exp((\alpha - 1)(\alpha \epsilon - \rho))}{\alpha - 1} \left( 1 - \frac{1}{\alpha} \right)^\alpha.$$

### 2.2. DP Mechanisms

To achieve DP in different scenarios, various mechanisms have been proposed, such as the Gaussian mechanism [23] and the exponential mechanism [24]. We briefly

introduce them in this section. Before introducing DP mechanisms, we first need to define sensitivity:

**Definition 3** (Sensitivity). Let  $f : \mathcal{D} \rightarrow \mathcal{R}^k$  be a vector-valued function of the input data, then the  $\ell_2$  sensitivity of  $f$  is defined as,

$$\Delta_f = \max_{D \simeq D'} \|f(D) - f(D')\|_2$$

**Gaussian Mechanism.** Gaussian Mechanism (GM) [23], which directly adds Gaussian noise to function results, has been widely used to achieve  $\rho$ -zCDP. Specifically, let  $f$  be a vector-valued function of the input data. The GM adds i.i.d. Gaussian noise with scale  $\sigma\Delta_f$  to each entry of  $f$ ,

$$\mathcal{A}(D) = f(D) + \sigma\Delta_f \mathcal{N}(0, \mathbb{I}), \quad (1)$$

where  $\mathcal{N}(0, \mathbb{I})$  refers to the standard Gaussian distribution. The zCDP guarantee of GM is given by the proposition 4.

**Proposition 4.** The Gaussian Mechanism satisfies  $\frac{1}{2\sigma^2}$ -zCDP.

**Exponential Mechanism.** Let  $q_i$  be a score function for all  $i \in C$ . The exponential mechanism (EM) [5], [12], [24] selects a candidate  $r$  according to the following distribution:

$$\Pr[\mathcal{A}(D) = r] \propto \exp\left(\frac{\epsilon}{2\Delta} \cdot q_r(D)\right), \quad (2)$$

where  $\Delta = \max_{i \in C} \Delta(q_i)$ . The zCDP guarantee of EM is provided by proposition 5

**Proposition 5.** The Exponential Mechanism satisfies  $\frac{\epsilon^2}{8}$ -zCDP.

### 2.3. DP Tabular Data Synthesis

Firstly, we introduce some key concepts of DP tabular data synthesis. The first one is a formal definition of the tabular dataset.

**Definition 4** (Tabular Dataset). A tabular dataset  $D$  is defined as a set of  $N$  record tuples  $\{x_1, \dots, x_N\}$ . Each record contains  $d$  values, representing its entries across  $d$  attributes  $\{A_1, \dots, A_d\}$ .

Generally, we assume that the set  $\Omega_i$  of possible values of each attribute  $A_i$ , namely the domain of this attribute, is public. The domain for the dataset is defined by  $\Omega = \Omega_1 \times \dots \times \Omega_d$ . Another important concept related to tabular data is marginal, defined as below.

**Definition 5** (Marginal). Let  $r \in \{1, \dots, d\}$  be a subset of the attribute index, and we have a corresponding dataset  $D_r \subseteq D$  with domain  $\Omega_r = \prod_{i \in r} \Omega_i$ . A marginal  $M$  is a vector of frequency counts for each value in  $\Omega_r$ . More formally, we define  $M[t] = \sum_i \mathbb{1}\{x_i^r = \Omega_r[t]\}$ , where  $x_i^r$  is the  $i$ -th record in  $D_r$ .

Marginal is widely applied in statistical methods [5], [6], [9], [25], and has been proven effective in data representation for tabular data synthesis. We define the DP tabular data synthesis task in Definition 6.

TABLE 1: Related work for DP tabular data synthesis. Model column contains the generative model used for data generation; DP mechanism refers to how the algorithm involves DP into it; feature column includes the data feature used to capture distribution information (if used).

Algorithm	Model	DP Mechanism	Feature
AIM (SOTA) [5]	PGM [26]	Feature DP	Marginal
DPGAN [16]	GAN	Gradient DP	-
dp-GAN [27]	GAN	Gradient DP	-
GS-WGAN [14]	GAN	Gradient DP	-
DP-CTGAN [22]	GAN	Gradient DP	-
DP-TabDDPM [28]	Diffusion	Gradient DP	-
SynLM [29]	LLM	Gradient DP	-
DP-LLMGen [17]	LLM	Gradient DP	-
PATE-GAN [21]	GAN	Feature DP	Teacher Voting
DP-MERF [13]	NN	Feature DP	Fourier Feature
GEM [12]	NN	Feature DP	Marginal Query

**Definition 6** (DP Tabular Data Synthesis). DP tabular data synthesis is defined as the problem of synthesizing an artificial tabular dataset  $D'$  similar to the sensitive dataset  $D$  with DP guarantee. The two datasets are considered similar if for any  $r$ -way marginals, where  $r \in \{1, \dots, d\}$ , the distance (e.g.,  $\ell_1$  distance) between the marginal from  $D'$  and its counterpart from  $D$  should be minimized.

## 3. Related Work and Motivation

In this section, we review several related works on DP tabular data synthesis, including the state-of-the-art method, AIM, and some NN-based approaches. These approaches are summarized in Table 1. Following this overview, we will critically discuss their limitations, thereby establishing the motivation and providing guidance for our work.

### 3.1. Related Work

**AIM.** AIM is a highly effective algorithm for DP tabular data synthesis, which has been recognized as the *state-of-the-art* solution in various studies [5], [11]. It works by iteratively selecting and privatizing low-dimensional marginals, and then integrating them into a private-probabilistic graphical model (PGM) [26]. In PGM, based on the selected marginals, attributes are grouped into several cliques  $\{C_1, \dots, C_k\}$ , each of which intersects with the previous clique on  $S_i$  (where  $i \in \{2, \dots, k\}$ ). Then, by estimating the distribution of each clique, PGM can model the joint distribution by factorizing it across a chain of cliques:

$$\hat{p} = \Pr[C_1] \cdot \prod_{i=2}^k \Pr[C_i \setminus S_i \mid S_i].$$

AIM's strength stems from two key design aspects: (1) adaptive marginal selection for efficient information extraction, and (2) PGM's ability to estimate the joint distribution with a limited number of marginals under the conditional independence assumption across the cliques.

**Gradient-DP NN-based Method.** This category refers to the NN-based methods that apply DP Stochastic Gradient

Descent (DP-SGD) [30] to train generative models. These approaches are straightforward: training standard tabular generative models using DP-SGD to ensure privacy. Early efforts include DPGAN [16] and dp-GAN [27], which applied DP-SGD to GAN architectures originally designed for images but adaptable to tabular data. Subsequent work has focused on improving model architectures and training mechanisms. For instance, DP-CTGAN [22] introduces conditional generators for better attribute distribution learning, while GS-WGAN [14] reduces noise by privatizing only aggregated critic gradients. This paradigm has been extended to diffusion models [11], [28] and large language models [17], [29]. However, as LLMs’ performance may be confounded by pre-training on extensive public datasets, which are unknown to us and can lead to privacy concerns and unfair comparisons, we omit further discussion of those LLM-based methods.

**Feature-DP NN-based Method.** Feature-DP NN-based methods first extract and privatize statistical features, then train models on these noisy features rather than the original data [12], [13], [21]. This approach requires only a single noise addition step applied to feature values, avoiding the high-variance noise accumulation from multiple DP-SGD iterations. The general framework can be formulated as:

$$\min_{G \in \mathcal{G}} \sum_{i=1}^k \mathcal{L}(f_i(D), \hat{f}_i(\hat{D})), \text{ s.t. } \hat{D} \leftarrow G \quad (3)$$

Here,  $\{f_1, \dots, f_k\}$  are feature extractors mapping datasets to pre-defined feature spaces. The loss measures distances between features of the real dataset  $D$  and the synthetic dataset  $\hat{D}$ , guiding the training of the generator  $G$ . Representative methods include PATE-GAN [21], which uses noisy voting from teacher discriminators to train a student discriminator, which further guide the data generator; DP-MERF [13], which constructs loss functions using random Fourier features mean embedding; and GEM [12] leverages iteratively selected marginal queries that provides a scalar answer to a specific local distributional question (e.g., the probability of a certain value combination of a subset of attributes), achieving superior performance among neural network-based methods [11].

### 3.2. Motivation

Section 3.1 provides an overview of various solutions for DP tabular data synthesis. In this section, we will elaborate on their respective limitations. This analysis of existing shortcomings directly motivates our work.

**AIM: Prohibitive Cost for Complex Correlations.** Although AIM’s design brings superior synthesis utility, it also introduces a critical vulnerability: its inability to manage complex correlations. As data dependencies become more complex, more marginals are required, causing an exponential expansion of the cliques’ domain size. Consequently, AIM must omit certain dependencies, even highly informative ones, to avoid prohibitive costs.

Figure 1 provides two conceptual examples to illustrate this challenge. The first example considers a dataset with

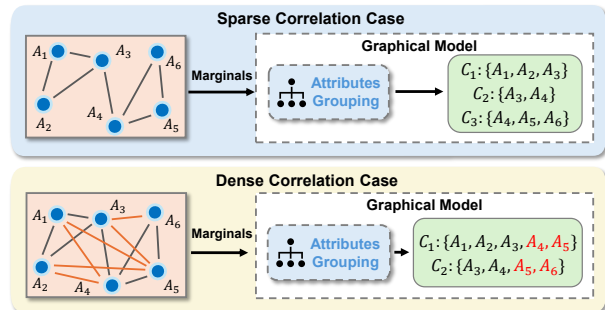


Figure 1: Examples of PGM’s attributes grouping process. The blue nodes represent attributes, and the edges between nodes are marginals. The densely correlated dataset leads to cliques with larger domain sizes.

six attributes, where only seven marginals are identified (depicted in the upper graph of Figure 1). PGM constructs a graph model that groups all attributes into three modest cliques, each containing at most three attributes. Those unselected correlations can be inferred from measured marginals. For instance, we can infer  $\Pr(A_2, A_4)$  as:

$$\Pr(A_2, A_4) \approx \sum_{A_3} \Pr(A_2|A_3) \cdot \Pr(A_4|A_3) \cdot \Pr(A_3)$$

However, in the second example, more strong correlations exist in this dataset, violating the conditional independence assumption (illustrated in the bottom figure of Figure 1). In this situation, PGM is forced to generate larger cliques, such as those containing four to five attributes, to accommodate these new dependencies. Assuming a domain size of 100 for each attribute, the state space of the largest clique thus increases from  $10^6$  to  $10^{10}$ . This exponential growth renders the estimation of the clique’s probability distribution computationally infeasible.

**Existing NN-based Methods: Imperfect Algorithmic Designs.** Given the limitations of AIM, neural networks emerge as a promising solution due to their inherent capacity to approximate complex data distributions by directly generating samples. However, the algorithmic designs of existing NN-based methods also have their weaknesses, reflected in their significant performance gap compared to statistical methods like AIM in prior benchmarks [10], [11].

For gradient-DP methods, while they are constructed on strong generative models [28], [31], DP-SGD limits the number of optimization steps due to the cumulative privacy cost and degrades gradient accuracy through clipping and noise addition, bringing difficulty to capture data distributions accurately [10], [11]. The feature-DP methods also have their drawbacks. For instance, the voting result in PATE-GAN [21] provides only a coarse, binary “yes or no” judgment. DP-MERF [13] employs a random Fourier feature mean embedding, which requires infinite dimensions to capture the distribution accurately. However, in practice, we can only use a relatively small dimension to control the DP noise level. Finally, although GEM [12] uses marginal queries to obtain stronger feature representativeness, the

TABLE 2: Comparison of existing works. “✓” denotes that the work includes this property; “✗” denotes that the work does not have this property, indicating its limitation.

Work	Handle Complex Correlations	Strong Distribution Capture Ability	Comprehensive Evaluation
AIM	✗	✓	✗
NN-based methods	✓	✗	✗
Our Work	✓	✓	✓

measurements of multiple disjoint queries on the same marginal consume budget separately, whereas using the complete marginal could share a single allocation. GEM’s fixed-round selection strategy also limits performance: even with sufficient remaining budget, the algorithm cannot select more features to improve the model.

**Prior Evaluations: An Incomprehensive Scope.** Finally, we discuss the limitations within the evaluations in existing evaluations for DP tabular synthesis methods [5], [6], [9], [10], [11], [12]. Existing evaluations overlook the influence of correlations’ distribution on synthesis algorithms. They are predominantly conducted on sparsely correlated data, where attributes exhibit weak dependencies. This characteristic allows datasets to be naturally partitioned into small cliques, thereby preventing a robust validation of neural networks’ theoretical advantages on complex correlation structures, such as densely correlated datasets.

We summarize the aforementioned limitations in Table 2. These limitations reveal a critical insight: the consensus on AIM’s superiority is likely incomplete and confined to simple benchmarks, as its performance is expected to degrade on more intricately correlated datasets. Meanwhile, neural networks, a natural alternative in these difficult scenarios, currently lack sufficiently robust algorithmic designs to be effective. To address these challenges, our future work will focus on two efforts: (1) developing a powerful NN-based algorithm, and (2) conducting comprehensive experiments with fine-grained comparisons and including those challenging, densely correlated datasets.

## 4. MargNet

In Section 3, we identified key limitations of existing works and outlined directions for further efforts. Among these, the foremost priority is developing improved algorithms. In this section, we present MargNet, a new method designed to address this challenge.

### 4.1. Algorithm Overview

Before introducing our method in detail, we describe the design intuition and provide an algorithm overview. Recall from Section 3 that existing feature-DP methods have several drawbacks, such as imperfect features and suboptimal privacy utilization. Considering these problems, we propose MargNet in Algorithm 1, which is based on marginal feature and utilizes an adaptive selection strategy, illustrated in Figure 2.

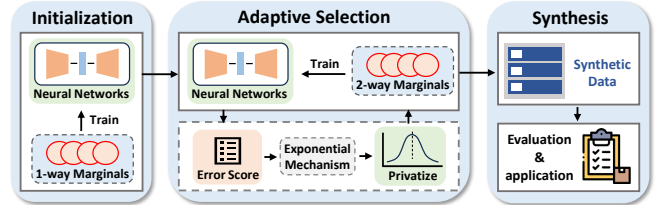


Figure 2: A brief illustration of MargNet. First, the model is initialized with all one-way marginals. Then, an adaptive marginal selection and model fitting step is conducted, which returns the model to synthesize data.

MargNet consists of four main steps: hyperparameter initialization (line 1), model initialization (lines 2–6), marginal selection and model update (line 7), and synthesis (line 8). First, we split the total budget into two basic units:  $\rho_s$  for selection and  $\rho_m$  for measurement, where  $c$  is a hyperparameter constraining the maximum number of selection steps (see Appendix C). Then, following prior works [5], [6], [32], we split a small proportion of privacy budget to measure all one-way marginals and fit the model as a warm-up step. After these preparations, we consider utilizing the necessary two-way marginals to capture the correlations in the dataset, which leads to further adaptive marginal selection and model update. Finally, with a well-trained model  $G$ , we can generate data from it.

This overview leaves two critical design questions unaddressed. The first is the specific strategy used for adaptively selecting the marginals. The second is the precise mechanism by which the model  $G$  is trained and updated based on these selections. In Section 4.2 and Section 4.3, we will provide a detailed description of our algorithmic design for each of these two essential steps.

### 4.2. Adaptive Marginal Selection

Various previous studies [5], [6], [7], [9], [12] have proposed iterative mechanisms to select features. The most successful one is the adaptive mechanism used in AIM [26]. Based on these previous works, we propose an adaptive marginal selection framework more tailored to generative neural networks, as shown in Algorithm 2.

The primary workflow of Algorithm 2 is an iterative process that repeatedly selects marginals and fits the model till all privacy budget is used. First, we initialize the privacy consumption accountant  $\rho_{\text{used}}$  (line 1). After that, we conduct the adaptive selection. In each iteration, we first apply an exponential mechanism to select marginal  $M_i$  with a commonly-used score function  $q_i$  [5], [6]:

$$q_i = r_i \left( \|M_i(G^{k-1}) - M_i\|_1 - n_i / \sqrt{\pi \rho_m} \right) \quad (4)$$

This score can be interpreted as the expected improvement in estimating  $M_i$  after we select it (estimation improvement minus noise error). The first term  $\|M_i(G^{k-1}) - M_i(D)\|_1$ , where  $M_i(G^{k-1})$  and  $M_i$  are estimated marginal by  $G^{k-1}$  and real marginal, respectively, is the expected improvement we can achieve after selecting  $M_i$ , regardless of DP noise.

---

**Algorithm 1:** MargNet

---

**Input:** Dataset  $D$ , total privacy budget  $\rho$ , hyperparameter  $c$ .

**Output:** sampled data  $D'$ .

- 1 Set  $\rho_s = 0.1\rho/c$  and  $\rho_m = 0.9\rho/c$ ;
- 2 Initialize model  $G$  parameterized by  $\theta$ ;
- 3 Measure all one-way marginals  $\tilde{M}_1^1, \dots, \tilde{M}_d^1$  with budget  $\rho_m$ ;

$$\tilde{M}_i^1 = M_i^1 + \mathcal{N}\left(0, \frac{1}{\sqrt{2\rho_m}}\right);$$

- 4  $S = \{\tilde{M}_1^1, \dots, \tilde{M}_d^1\}$ ;
  - 5  $\rho_{\text{total}} = \rho - d\rho_m$ ;
  - 6 Train model  $G$  on  $S$  by Algorithm 3;
  - 7 Adaptively select marginals into  $S$  and update model  $G$  with  $\rho_{\text{total}}$  by Algorithm 2;
  - 8 Generate  $D'$  from  $G$ ;
  - 9 **return**  $D'$ .
- 

However, our measurement should be privatized by DP noise. We reduce it by  $n_i/\sqrt{\pi\rho_m}$ , which is the expected  $\ell_1$  norm of DP noise. Here  $n_i$  is the size of  $M_i$  and  $\rho_m$  is the privacy budget for measurement;  $r_i$  is a hyperparameter which is set to 1.0 in our experiments for simplicity. The following theorem [5] gives the sensitivity of  $q_i$ .

**Theorem 1.** The sensitivity of the score function  $q_i$  defined in Equation (4) is  $r_i$ .

After we obtain the newly selected marginal from the exponential mechanism, we privately measure it with Gaussian noise and train the model on all selected marginals (lines 6–8). This part will be introduced in detail in Section 4.3.

The final step of each iteration is to update the privacy accountant and adjust the budget allocation (lines 9–14). We first add  $\rho_s$  and  $\rho_m$  to  $\rho_{\text{used}}$  to track cumulative consumption. Then, we update the per-iteration budget allocation  $\rho_s$  and  $\rho_m$  for future rounds (lines 10–11).

This update mechanism balances two competing objectives: allocating more budget per iteration improves marginal selection reliability and reduces total iterations, while distributing budget across multiple iterations enables better noise management through Gaussian noise additivity. Prior work [5] suggests that when model improvement from selecting  $M_k$  falls below the expected noise error, budget increases may be beneficial:

$$\|M_k(G^k) - M_k(G^{k-1})\|_1 < n_k/\sqrt{\pi\rho_m} \quad (5)$$

This condition indicates that either (1) the selected marginal itself yields limited new information, or (2) the current budget allocation produces measurements dominated by noise rather than signal. In these cases, increasing budget division can help stabilize marginal selection to choose more informative candidates and measure marginals more accurately.

We refine this into our update criterion by adding a first-time selection constraint: budget increases occur only

---

**Algorithm 2:** Adaptive Selection Framework

---

**Input:** Dataset  $D$ , initialized model  $G$ , initialized marginal set  $S$ , privacy budget  $\rho_{\text{total}}$ , budgets allocated for selection and measurement  $\rho_s, \rho_m$ .

**Output:** Generative model  $G^k$ .

- 1  $\rho_{\text{used}} = 0, G^0 = G$ ;
  - 2  $k = 0$ ;
  - 3 **while**  $\rho_{\text{used}} < \rho_{\text{total}}$  **do**
  - 4      $k = k + 1$ ;
  - 5     Select two-way marginal  $M_k$  using exponential mechanism with budget  $\rho_s$  and score:
 
$$q_i = r_i (\|M_i(G^{k-1}) - M_i\|_1 - n_i/\sqrt{\pi\rho_m})$$
  - 6      $\tilde{M}_k = M_k + \mathcal{N}\left(0, \frac{1}{\sqrt{2\rho_m}}\right)$ ;
  - 7      $S = S \cup \{\tilde{M}_k\}$ ;
  - 8     Obtain model  $G^k$  by training  $G^{k-1}$  on  $S$  by Algorithm 3;
  - 9      $\rho_{\text{used}} = \rho_{\text{used}} + \rho_s + \rho_m$ ;
  - 10    **if**  $\|M_k(G^k) - M_k(G^{k-1})\|_1 < n_k/\sqrt{\pi\rho_m}$  and  $M_k$  is selected for the first time **then**
  - 11      Double  $\rho_m$  and  $\rho_s$ ;
  - 12    **if**  $\rho_{\text{used}} + \rho_s + \rho_m \geq \rho$  **then**
  - 13       $\rho_s = 0.1(\rho_{\text{total}} - \rho_{\text{used}})$ ;
  - 14       $\rho_m = 0.9(\rho_{\text{total}} - \rho_{\text{used}})$ ;
  - 15    Train model  $G^k$  on  $S$  by Algorithm 3 with  $\beta = \text{False}$ ;
  - 16 **return**  $G^k$ .
- 

when both Equation (5) holds and the marginal is selected for the first time. This design is based on the assumption that if a selected marginal is truly unsuitable or if measurement error is prohibitively high, these issues manifest upon first selection. By restricting budget increases to first-time selections, we avoid repeated escalation for the same marginal, instead preserving budget for additional iterations to capture more correlations, enhancing the ability to deal with complex datasets.

This budget division update step is followed by a judgment of whether the remaining budget,  $\rho_{\text{total}} - \rho_{\text{used}}$ , is enough for the next iteration. If not, we allocate all the remaining budget to the next round, thereby terminating the iterations because no budget remains. After the selection iterations terminate, we fit all marginals and return the model for data synthesis (lines 15–16).

### 4.3. Training with Marginals

The second challenge is how to effectively train a neural network using the selected marginals. To address this, we design a differentiable training pipeline (Algorithm 3), inspired by feature-fitting techniques in prior work [12], [13].

The workflow of Algorithm 3 iteratively updates model  $G$  through gradient descent. First, we need to count the

---

**Algorithm 3:** Marginal Training

---

**Input:** Model  $G$  parameterized by  $\theta$ , iteration  $T$ , learning rate  $r$ , a set of marginals  $S$ , loss weight parameter  $w_{1:|S|}$ .

**Output:** Model after training  $G$ .

```

1  $t = 0$ ;
2 while  $t < T$  do
3    $z \leftarrow$  Random Distribution;
4    $D' = G(z)$ ;
5   Compute loss:
      
$$\mathcal{L}(\theta, S) = \sum_{i=1}^{|S|} w_i \left\| M_i(D') - \tilde{M}_i \right\|_F^2$$

      ;
6   Calculate gradient:  $g_\theta = \nabla_\theta \mathcal{L}(\theta, S)$ ;
7   Update model  $G$  with  $g_\theta$  and learning rate  $r$ ;
8    $t = t + 1$ ;
9 return  $G$ .
```

---

frequency of each value in the marginal distribution from the model’s output while maintaining differentiability for backpropagation. To achieve this, we generate a batch of samples from  $G$  where categorical values are represented as soft probability distributions, analogous to one-hot encodings but with continuous probabilities rather than discrete 0/1 values. We then average these soft probabilities across the batch to obtain the empirical frequency for each cell in the marginal. Finally, we scale these frequencies to derive the marginal estimation  $M_i(D')$ .

Second, we apply a weighted loss function. The weights  $w_i$  are designed with two considerations: (1) since marginals are measured with varying noise levels, we assign higher weights to more reliable measurements (lower noise); (2) as we accumulate more marginals through iterations, the signal from each newly added marginal becomes diluted among an increasing number of training targets, requiring amplified weights to ensure effective learning. We formulate the weights as:

$$w_i \propto \begin{cases} \sqrt{\rho_{m,i}}, & M_i \text{ is not newly selected} \\ d\sqrt{\rho_{m,i}}, & M_i \text{ is newly selected} \end{cases} \quad (6)$$

where  $\sqrt{\rho_{m,i}}$  is inversely proportional to the noise standard deviation in measuring  $M_i$ . For newly selected marginals, we multiply the base weight by  $d$  (the dataset dimensionality) to compensate for signal dilution as the total number of training targets grows. Detailed discussion of this design is provided in Appendix C.

#### 4.4. Privacy Guarantee

This subsection gives the privacy guarantee of MargNet. It is mainly based on the privacy filter [5], [33], [34], [35], which can guarantee DP (zCDP) under an adaptive strategy.

**Theorem 2.** For any input  $\rho \geq 0$  and other parameters, Algorithm 1 satisfies  $\rho$ -zCDP.

When initializing the model, we measure  $d$  one-way marginals with budget  $\rho_m$ . This step satisfies  $d\rho_m$ -zCDP by the composition theorem. Due to our setting, we know that  $d\rho_m < \rho$ , which means we do not overspend the privacy budget. Then, in Algorithm 2, marginal selection and measurement steps occur spontaneously. Because we limit the used budget not to exceed the total budget  $\rho_{\text{total}}$  (line 3), and use all the remaining budget if it is not enough for the next round (line 12–14), the Algorithm 2 satisfies  $\rho_{\text{total}}$ -zCDP by the property of privacy filter [35]. Note that referring to line 6 of Algorithm 1, we have  $\rho = \rho_{\text{total}} + d\rho_m$ . Therefore, we can claim that Algorithm 1 satisfies  $\rho$ -zCDP.

## 5. Theoretical Evaluation

Before we move to experimental evaluation, in this section, we evaluate MargNet’s theoretical fitting error. We will conduct our analysis from two aspects: selected marginal errors and unselected marginal errors.

### 5.1. Selected Marginal Errors

The simpler case is when a marginal is selected and measured. We assume that the index set  $I_s$  contains indices of all selected marginals. For any  $i \in I_s$ , the selected marginal  $M_i$  is measured as  $\tilde{M}_i$ , and correspondingly fitted as  $\hat{M}_i$  by any model. The total error of selected marginals can be formulated as

$$\mathcal{L}_s(G) = \sum_{i \in I_s} \|M_i - \hat{M}_i(G)\|_F^2 \quad (7)$$

Here,  $\hat{M}_i(G)$  is achieved by first generating a batch of samples and counting the frequency of each value. This raises a problem that we are using a small number of samples to estimate a highly complex matrix, which can lead to an inherent error. Based on this intuition, we now give a lower bound on  $\mathcal{L}(G)$  in the subsequent theorem.

**Theorem 3.** Assuming that the theoretically optimal estimations of selected marginals  $M_1, \dots, M_{|I_s|}$  are formulated in two-order matrices, the total fitting error of all selected two-way marginals at MargNet’s any training batch has a lower bound

$$\mathcal{L}_s(G) \geq \sum_{i \in I_s} \left( \sum_{t=b+1}^{r(M_i)} \lambda_{i,t}^2 \right) \quad (8)$$

Here  $b$  is the batch size and  $\lambda_{i,t}$  is the  $t$ -th largest singular value of  $M_i$ .

The error identified in Theorem 3 stems from the limited sample space. This specific error is absent in PGM, as PGM directly fits the probability distributions of its cliques, ensuring their local representativeness. This highlights a fundamental trade-off: our approach simplifies the modeling to gain scalability to higher-dimensional cases, but introduces a systematic error in the process. In contrast, PGM’s more structured method avoids this sampling error, but at the cost of the computational constraints discussed previously.

Now, we discuss an upper bound guarantee of MargNet. Deriving a deterministic upper bound is challenging, as we make no assumptions about the optimization process. Therefore, following a similar approach to the analysis of AIM [5], we instead provide a confidence bound that is conditioned on the final, observed model error.

**Theorem 4.** Assuming that each selected marginal  $M_i$  is measured with Gaussian noise from privacy budgets  $\rho_m^j$  and trained with weight  $w_j$  for all  $j \in J_s^i$  (here  $J_s^i$  is used to demonstrate the case when a marginal is selected multiple times), we define an unbiased marginal for each  $i \in I_s$  as

$$\bar{M}_i \sim M_i + \mathcal{N}(0, \bar{\sigma}_i^2 \mathbb{I}), \text{ where } \bar{\sigma}_i = \left( \sum_{j \in J_s^i} \frac{w_j^2}{2\rho_m^j} \right)^{1/2}$$

The total fitting error of all selected two-way marginals at MargNet’s any training batch has an upper bound with probability  $1 - \sum_i \delta_i$ :

$$\mathcal{L}_s(G) \leq 2 \sum_{i \in I_s} \left( \left\| \bar{M}_i - \hat{M}_i(G) \right\|_F^2 + \sigma_i^2 F_{\chi_{n_i}^2}^{-1}(1 - \delta_i) \right) \quad (9)$$

Here,  $F_{\chi_{n_i}^2}^{-1}$  is the inverse cumulative distribution function of the Chi-squared distribution with  $n_i$  degrees of freedom.

Equation (9) consists of two terms. The first term is the discrepancy between the marginal predicted by the model and our defined unbiased estimator, which is an observable quantity at any time. The second term represents the error introduced by the DP noise. The proof of Theorem 4 is provided in Appendix B.

## 5.2. Unselected Marginal Errors

For those unselected marginals, we investigate their total estimation error as

$$\mathcal{L}_u(G) = \sum_{i \in I_u} \left\| M_i - \hat{M}_i(G) \right\|_1$$

A notable difference between this error and the selected marginal error is that we consider  $\ell_1$  error here. This is because our further analysis and proof rely on the score function in the exponential mechanism (Equation (4)), which is based on  $\ell_1$  error. McKenna et al. [5] have discussed this issue under AIM’s adaptive framework. The main idea of their analysis is that, even though we have not selected some marginals, we can still obtain some estimation because we expect unselected marginals to have minor errors due to the exponential mechanism. Based on their work, we can obtain a bound on the unselected marginal error of MargNet from Theorem 5. The detailed proof is included in Appendix B.

**Theorem 5.** In MargNet, assuming that we have conducted  $K$  selection steps and selected marginal  $M_\theta$  from the candidate set  $C$  in the final round. The index set for unselected marginals is  $I_u$ . For any unselected marginal  $M_i$ , the estimations of it by the model  $G$  and intermediate model  $G^{K-1}$

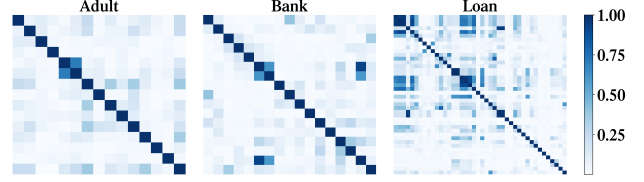


Figure 3: Heatmap on absolute values of pairwise correlations in the real-world datasets. The darker the color, the stronger the correlation.

are  $\hat{M}_i$  and  $\hat{M}_i^{K-1}$ , respectively. We define

$$B_{i,K} = \frac{r_\theta}{r_i} \left\| M_\theta - \hat{M}_\theta^{K-1} \right\|_1 + \frac{n_i r_i - n_\theta r_\theta}{r_i \sqrt{\pi \rho_s^K}} + \frac{\Delta_q}{r_i \sqrt{2 \rho_s^K}} \log \frac{|C|}{\delta} \quad (10)$$

Here, the definition of  $r_i$ ,  $r_\theta$ ,  $n_i$ ,  $n_\theta$  is the same as that in Equation (4);  $\rho_s^K$  is the value of  $\rho_s$  in the last selection iteration;  $\delta$  is a fixed parameter. Then with more than probability  $1 - \sum_i \delta$ , we have

$$\mathcal{L}_u(G) \leq \sum_{i \in I_u} \left( B_{i,K} + \left\| \hat{M}_i^{K-1} - \hat{M}_i \right\|_1 \right) \quad (11)$$

There are two terms in Equation (11) that are related to model itself. The first term is  $\left\| M_\theta - \hat{M}_\theta^{K-1} \right\|_1$ . We can understand it as how well we estimate  $M_\theta$  before the last selection round, which is further determined by which marginals we selected before and how we fit them. The second one is  $\left\| \hat{M}_i^{K-1} - \hat{M}_i \right\|_1$ , which is the difference in the estimation of  $M_i$  between the final model and the last model. We can assume it to be small, especially when  $K$  is large and the model converges to a stable point [5].

## 6. Experiments

### 6.1. Sparse Correlation Experiments

In the real world, most datasets contain sparse correlations. This case is often tested in previous experiments [5], [6], [7], [10], [11]. Therefore, we first conduct experiments on these datasets in this section.

**6.1.1. Experimental Settings.** We introduce our settings for sparse correlation experiments in three aspects: datasets, baselines, and metrics.

**Datasets.** We select three datasets, which have been widely employed by various previous works [6], [11], [36], [37], as shown in Table 3. In Figure 3, we plot the absolute values of pairwise correlations within these datasets in a heat map form. Darker colors mean stronger correlations. From these figures, most of the pairwise correlations are weak (correlation  $< 0.5$ ). This figure shows that all these datasets are sparsely correlated.

**Baselines.** For MargNet, we keep the generator structure the same as the generators of GEM and DP-CTGAN. Detailed information about hyperparameter settings is included in Appendix C. We select AIM, GEM, DP-MERF,

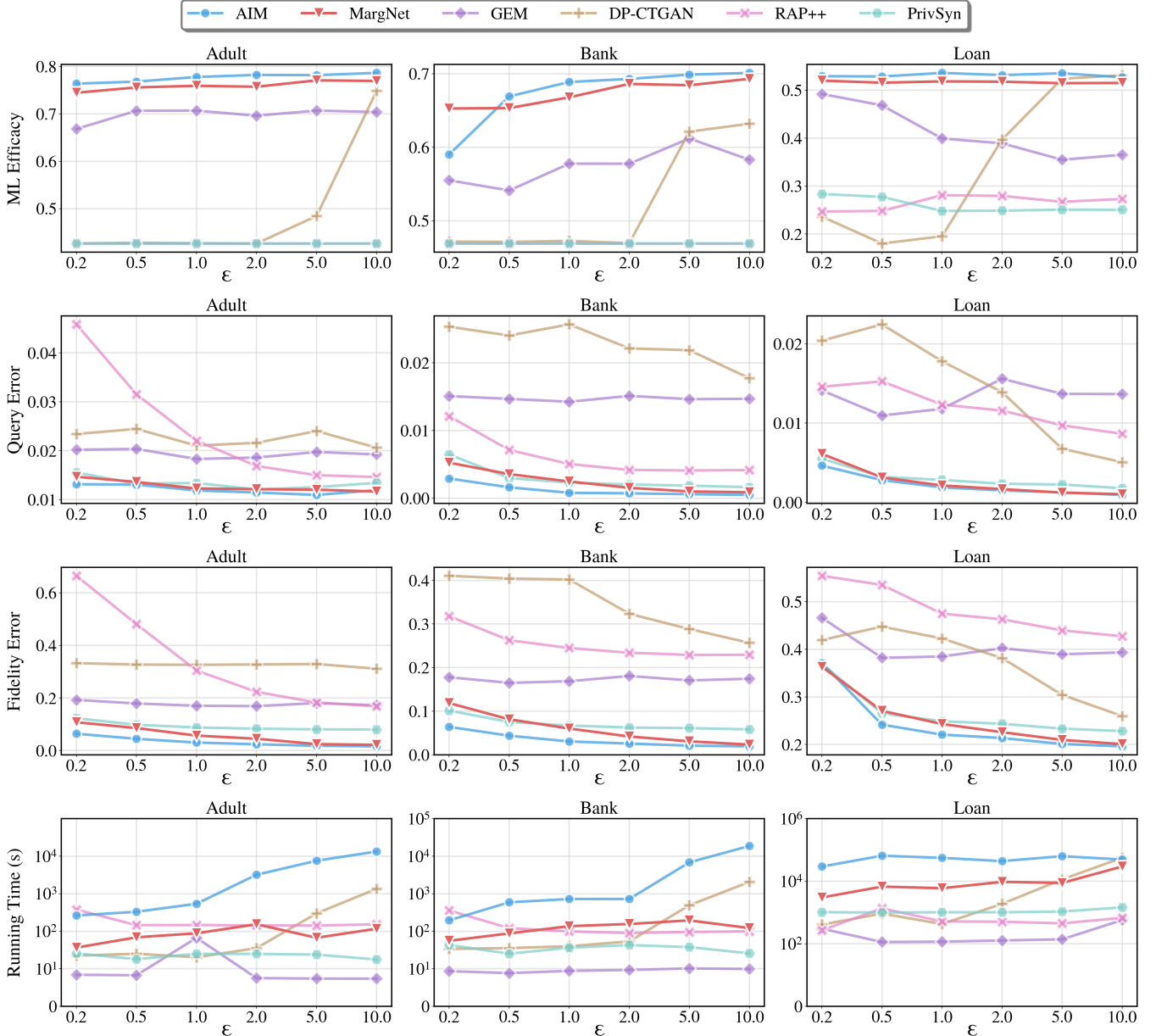


Figure 4: Evaluation results (machine learning efficacy, query error, and fidelity error) on sparsely correlated datasets. The three columns of figures depict the results on three datasets (Adult, Bank, and Loan) from left to right, respectively.

TABLE 3: Summary of Real-world Datasets.

Name	#Records	#Attr	#Num	#Cat	Domain Size
Adult [38]	32384	15	2	13	2 - 41
Bank [39]	45211	16	6	10	2 - 6024
Loan [40]	134658	42	25	17	2 - 93995

DP-CTGAN, RAP++, PrivSyn, DP-TabDDPM as our baselines. Among these methods, AIM, RAP++, and PrivSyn are statistical methods. RAP++ and PrivSyn are evaluated to compare other statistical methods that do not achieve state-of-the-art with AIM and MargNet. The remaining methods

are neural network-based methods. Some methods, such as PATE-GAN [21], DP-GAN [27], have been proven ineffective [13], [22]. Other methods like PrivMRF [9] and RAP [37] are conceptually similar to some of our baselines. Therefore, we do not include them in our experiments. Our experimental plots do not include DP-TabDDPM and DP-MERF because of their relatively weak performance. We provide them in Appendix D.

**Metrics.** To make our evaluation more effective and comprehensive, we survey several past works [5], [6], [11], [41], and focus on most commonly used metrics. We also investigate other evaluation metrics like memory cost in Ap-

pendix D. Every reported metric is the average performance on five synthetic datasets by each method.

- *Machine Learning Efficacy.* We select one attribute as the label and use the other attributes as the input to train a machine learning model. The machine learning efficacy is obtained by testing this model on the real dataset. We use Catboost, xgBoost, and Random Forest models as the evaluation models, which have also been commonly used in previous works [11], [28], [41]. We only report the F-1 score in our experiments because other metrics like accuracy and AUC-ROC yield similar results.
- *Query Error.* The query error is obtained by comparing the results of linear queries on synthetic and real data. This metric can efficiently evaluate high-dimensional distribution similarity between synthetic and real data to test algorithms’ generalization ability. Here, we conduct query error evaluation on 3-way marginals.
- *Fidelity Error.* For low-dimensional distributions, directly comparing them is the most precise way for evaluation. We apply Total Variance Distance (TVD) as the fidelity error of 2-way marginals, which is also commonly used in previous benchmarks [5], [10], [11].
- *Time Efficiency.* Here, we utilize the execution time as the measurement of efficiency, which can determine algorithms’ practicality in real-world applications but is often overlooked by previous works.

**6.1.2. Experimental Results.** We plot the synthesis utility and time efficiency of different algorithms on three sparsely correlated datasets in Figure 4.

**MargNet consistently outperforms other neural network-based methods and several statistical methods in synthesis utility.** Aligning with what we claimed before, existing solutions for DP tabular synthesis, such as DP-CTGAN, which relies on DP-SGD, DP-MERF, and GEM that combine neural networks with low-dimensional statistics, face challenges. Under low privacy budgets (e.g.,  $\epsilon \leq 5.0$ ), we observe that DP-CTGAN, which relies on DP-SGD, becomes almost ineffective. While its utility improves with a larger budget, even at a high  $\epsilon = 10.0$  in our settings, its synthesis utility is still weaker than that of MargNet, especially in query error and fidelity error. This suggests that a general-purpose DP mechanism like DP-SGD is less effective for this task than MargNet’s more specialized architecture. Moreover, we can observe that the performances of GEM and DP-MERF are still inferior to MargNet, validating our analysis that these feature-DP neural network-based methods still have flaws in their algorithmic design.

In addition, MargNet also demonstrates performance that is superior to several statistical methods, such as PrivSyn and RAP++. While statistical methods are the traditional approach, our experiments show several such algorithms failing to exceed MargNet’s utility. We hypothesize this is because, unlike the SOTA AIM, they lack a sufficiently powerful data representation (like PGM) in their generation process or employ sub-optimal feature selection steps [11]. The key takeaway from these results is that a well-designed

TABLE 4: Summary of Gaussian Datasets.

Name	#Records	#Attr	#Num	#Cat	Domain Size
Gauss10	16000	10	10	0	16000
Gauss30	80000	30	30	0	80000
Gauss50	160000	50	50	0	160000

neural network like MargNet can outperform several specialized statistical algorithms. This strongly supports our conclusion that neural networks are a highly viable and competitive paradigm for DP tabular data generation.

**AIM still outperforms other methods in synthesis utility, but the gap with MargNet narrows as the privacy budget grows, while MargNet also demonstrates higher time efficiency.** Regarding utility, AIM shows superior performance on these sparsely correlated datasets. However, the utility gap between MargNet and AIM narrows as the privacy budget increases, with their performance becoming close at larger budgets (e.g.,  $\epsilon = 10.0$ ). We attribute this to the fact that AIM’s primary advantage, its efficient privacy budget utilization from conditional independence estimations, becomes less significant when the budget is enough to measure more marginals. Furthermore, we observe that MargNet is significantly more time-efficient than AIM on these datasets, achieving an average speedup of  $7\times$ .

## 6.2. Dense Correlation Experiments

Another type of dataset we discussed is densely correlated datasets, which contain denser relationships that are harder for algorithms to capture. We infer that in this case, PGM is likely to be overwhelmed by an excessive number of marginals, while neural networks are a more suitable choice. In this section, we focus on evaluating the performance of algorithms and investigating key issues on these datasets.

**6.2.1. Experimental Settings.** The baselines used in this section are kept the same as those in Section 6.1. Therefore, we omit the description of them. Here, we introduce the datasets and metrics employed in this experimental study.

**Dataset.** We consider some artificial datasets to better demonstrate the algorithms’ performance in densely correlated cases. We fix a covariance matrix and generate three multi-dimensional Gaussian-distributed datasets, as shown in Table 4. The pairwise correlations are set to 0.8 so that each dataset is a densely correlated dataset.

**Metrics.** For Gaussian distribution data, machine learning efficacy is not necessary because a combination of all pairwise relations completely determines the covariance matrix. Therefore, we consider query error and fidelity error as the evaluation metrics, as defined in Section 6.1.

**6.2.2. Experimental Results.** The quantitative evaluation results on densely correlated datasets are plotted in Figure 5.

**On densely correlated datasets, MargNet demonstrates superiority over other methods, especially in high dimensions.** In these situations, MargNet and AIM are the top

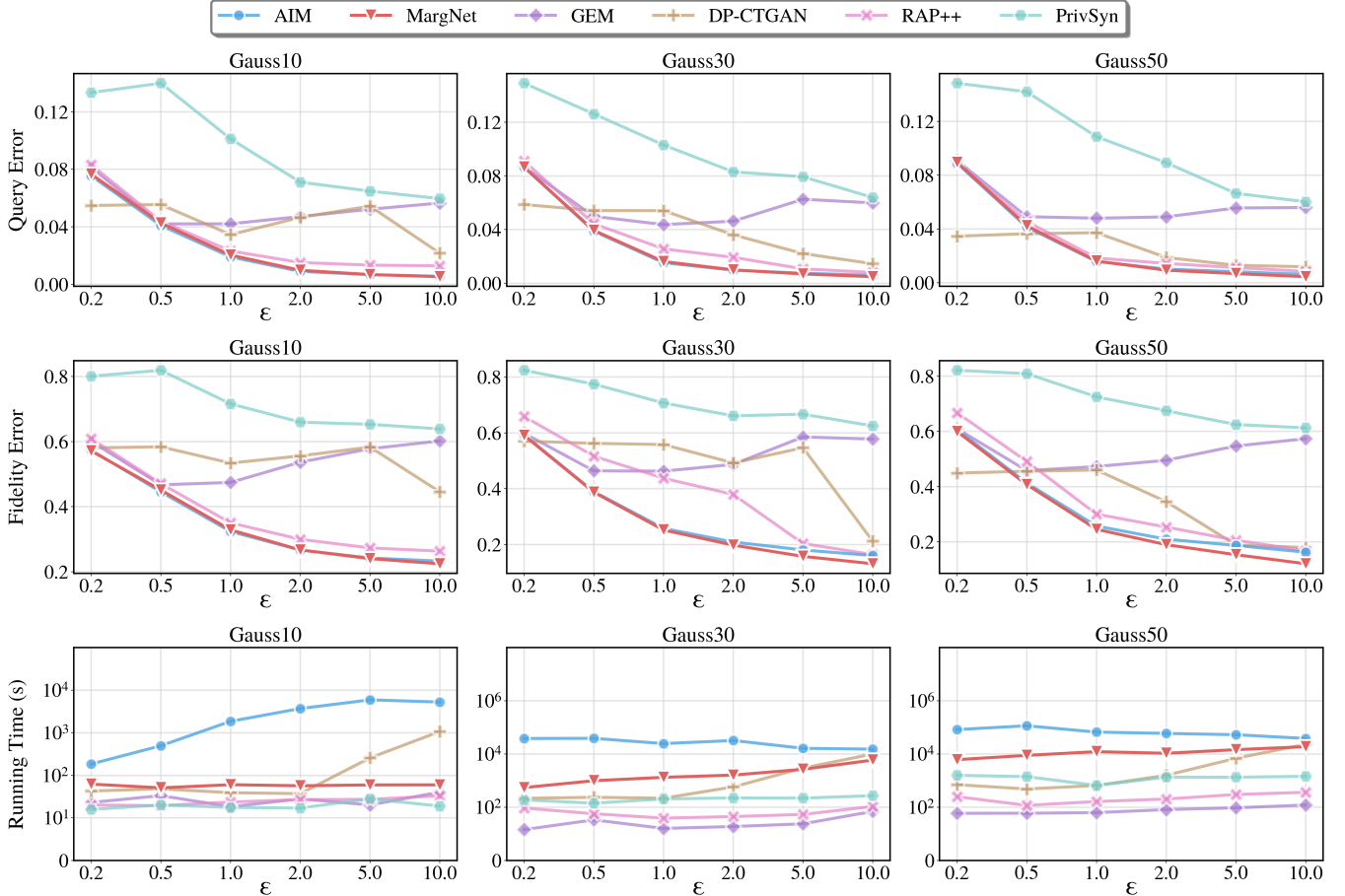


Figure 5: Different algorithms’ query errors, fidelity errors, and running time on densely correlated datasets. The three columns of figures depict the results on three datasets, Gauss10, Gauss30, and Gauss50 from left to right, respectively.

two algorithms. On Gauss10, their utility is nearly identical. On Gauss30 and Gauss50, MargNet surpasses AIM under sufficient privacy budgets (e.g.,  $\epsilon \geq 2.0$ ). On the Gauss50 dataset, with  $\epsilon = 10.0$ , MargNet achieved a fidelity error of 0.121, representing a reduction of approximately **26%** compared to AIM’s error of 0.163. We attribute this to a fundamental difference: PGM must decompose the joint distribution into local cliques and maintain small clique sizes for computational tractability, forcing it to omit some marginals. In contrast, MargNet can gradually capture all important marginals through adaptive selection without decomposition. We validate this in Section 6.3.

For DP-CTGAN, it outperforms other methods when  $\epsilon \leq 0.2$ . We attribute this to PrivTree discretization [42] under-splitting under low budgets, causing large discretization errors in other methods while DP-CTGAN outputs continuous results. This can be avoided using discretization methods requiring no privacy budget, such as  $k$ -uniform binning [11] (Appendix D). Similar to the findings in Section 6.1, DP-CTGAN’s performance improves substantially at  $\epsilon = 10.0$ , yet it remains inferior to MargNet in terms of synthesis utility.

Other findings align with Section 6.1. AIM suffers from

time inefficiency, requiring approximately 1, 7, and 17 hours on Gauss10, Gauss30, and Gauss50, respectively. Notably, AIM’s runtime remains stable on Gauss30 and Gauss50 but increases with privacy budget on Gauss10. This occurs because AIM constrains clique sizes: in high dimensions, this constraint is quickly reached even with an abundant budget, preventing larger cliques and reducing runtime, which also explains its inferior performance to MargNet in these cases.

### 6.3. Detailed Comparison

Section 6.1 and Section 6.2 provided a high-level comparison of utility and time efficiency for multiple algorithms, including MargNet and AIM. While these results align with our theoretical inferences, they do not offer a detailed validation of our underlying claims. Therefore, in this section, we conduct a deep investigation by answering two questions:

- Given an identical set of selected marginals, which model (NN or PGM) achieves higher fidelity when fitting those selected marginals and, crucially, when inferring the unselected marginals?

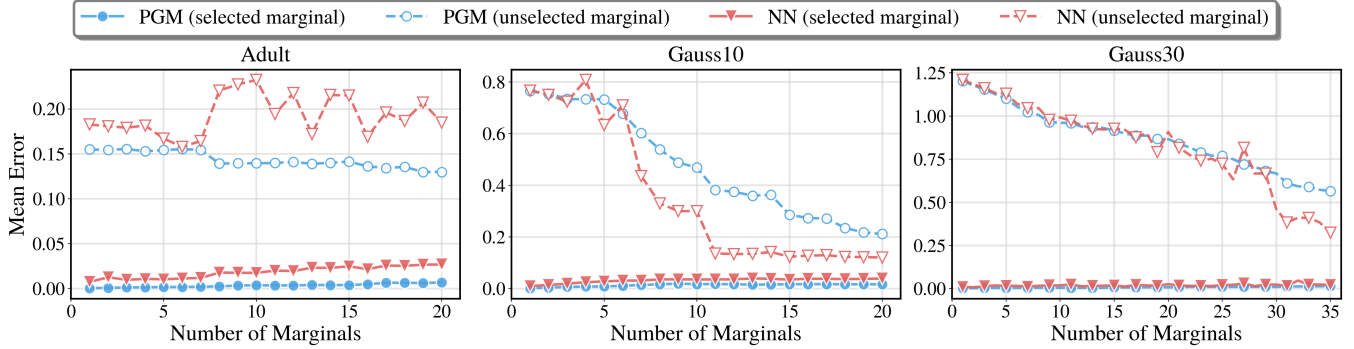


Figure 6:  $\ell_1$  distance error of selected and unselected marginals fitting by PGM and NN. The marginals are iteratively and randomly selected for fair comparison.

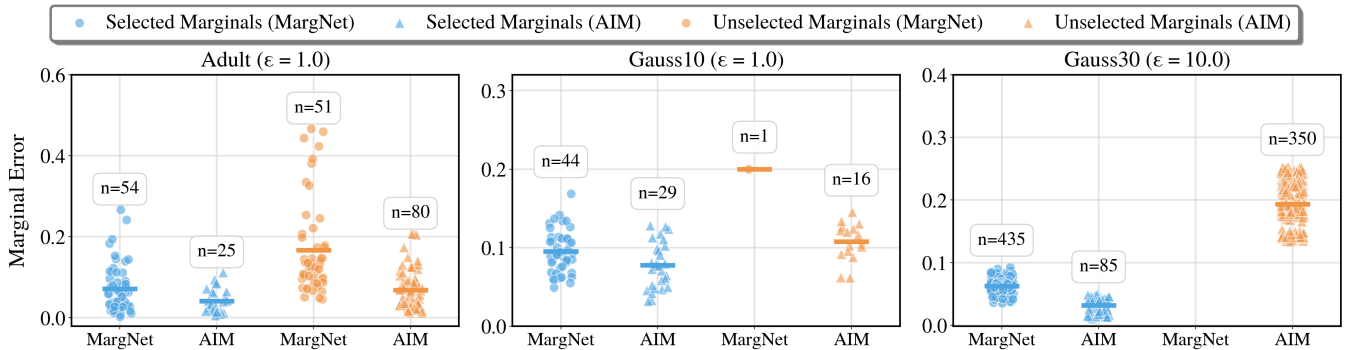


Figure 7:  $\ell_1$  distance error of selected and unselected marginals fitting by AIM and MargNet. The three results are obtained on the Adult and Gauss10 datasets under  $\epsilon = 1.0$ , and on the Gauss30 dataset under  $\epsilon = 10.0$ , respectively. Each point in this figure represents a marginal, and the horizontal short lines indicate the mean errors.

- In a practical setting, does MargNet effectively overcome the disadvantages AIM encounters when processing high-dimensional cliques?

**6.3.1. Experimental Settings.** Our experimental settings in this section are listed as follows.

**Datasets.** In this section, we mainly consider three datasets: Adult, Gauss10, and Gauss30 for simplicity.

**Baselines.** To compare the fitting ability of neural networks and PGM, we mainly consider AIM and MargNet.

**Metrics.** When comparing the fitting ability of PGM and neural networks, we focus on the  $\ell_1$  error of the two-way marginals. In experiments about fixed noise, we mainly focus on training loss and the metrics used to reflect utility in the previous sections.

**6.3.2. Experimental Results.** We plot our results in Figure 6 and Figure 7. In Figure 6, we initialize PGM and NN with all one-way marginals, and randomly select two-way marginals to fit the model. The number of two-way marginals serves as the x-axis. We record the average  $\ell_1$  error of both selected marginals and unselected marginals. In Figure 7, we consider three cases: (1) Adult under  $\epsilon = 1.0$ , where AIM outperform MargNet in synthesis utility; (2) Gauss10 under  $\epsilon = 1.0$ , where MargNet and AIM have similar performances; (3) Gauss30 under  $\epsilon = 10.0$ , where MargNet shows superior performance over AIM. We plot

the error of each marginal estimated by MargNet and AIM, respectively, to compare the actual fitting error.

**Given an identical set of marginals, PGM demonstrates stronger performance in fitting selected marginals, but the estimation error of unselected marginals depends on the dataset’s characteristics.** In Figure 6, PGM shows superior marginal estimation ability on the Adult dataset. Both its selected marginal error and unselected marginal error are lower than those of the neural network. We hypothesize that this is caused by the sparse correlations in the Adult dataset. This sparsity ensures that most unselected marginals can be accurately approximated either by assuming independence or through conditional independence estimations.

However, the situation is different on the Gauss10 and Gauss30 datasets. In these cases, PGM still exhibits more robust estimation of selected marginals, yet it is inferior to the neural network when inferring unselected marginals. We posit that this is due to the overly dense internal correlations within the data, which cause the (conditional) independence assumptions to fail.

**In practice, MargNet’s ability to select and fit a larger set of marginals enhances its model performance, which in some cases allows it to achieve lower marginal error compared with AIM.** Figure 7 demonstrates that, on the Adult dataset, even though MargNet selects more marginals, a certain number remain unselected, which corresponds to its

TABLE 5: Ablation study results on the Adult and Gauss10 dataset. ML eff., query err., and fidelity err. are the abbreviations of machine learning efficacy, query error, and fidelity error, respectively.

Dataset	$\epsilon$	Method	ML Eff. $\uparrow$	Query Err. $\downarrow$	Fidelity Err. $\downarrow$
Adult	0.2	MargNet-q	0.66	0.016	0.17
		MargNet-s	0.73	0.015	0.16
		MargNet	0.74	0.015	0.11
	1.0	MargNet-q	0.63	0.013	0.11
		MargNet-s	0.76	0.012	0.08
		MargNet	0.76	0.012	0.06
	10.0	MargNet-q	0.68	0.013	0.11
		MargNet-s	0.77	0.012	0.02
		MargNet	0.77	0.012	0.02
Gauss10	0.2	MargNet-q	-	0.076	0.59
		MargNet-s	-	0.077	0.58
		MargNet	-	0.077	0.57
	1.0	MargNet-q	-	0.022	0.40
		MargNet-s	-	0.021	0.33
		MargNet	-	0.020	0.32
	10.0	MargNet-q	-	0.017	0.44
		MargNet-s	-	0.006	0.23
		MargNet	-	0.005	0.22

larger fidelity error (as shown in Figure 4). On the Gauss10 dataset, while MargNet selects most marginals, AIM can also handle many of them due to the dataset’s relatively low dimensionality. On Gauss30, however, we observe that AIM can only afford a small proportion of marginals, leaving approximately 80% unselected. This results in its inferior performance compared to MargNet, which successfully handles all marginals. These results not only account for our experimental findings in the preceding two sections but also lend further support to the motivation behind this work.

## 6.4. Ablation Study

To identify which designs contribute to MargNet’s superior synthesis utility over prior neural network-based methods, we conduct an ablation study in this section. We systematically remove or modify key components of MargNet and compare the performances of these new algorithms with those of MargNet.

**6.4.1. Experimental Settings.** The metrics we use in this section are kept the same as Section 6.1. Here, we introduce the datasets and baselines.

**Datasets.** To keep the experiments simple yet representative, we conduct ablation studies on the Adult and Gauss10 datasets, which respectively represent the sparsely and densely correlated datasets. We set the privacy budget to  $\epsilon \in \{0.2, 1.0, 10.0\}$  to represent scenarios with limited, moderate, and abundant privacy budgets, respectively.

**Baselines.** In this section, we mainly consider comparing MargNet’s algorithm modules with those in state-of-the-art neural network-based algorithm, GEM [12], and propose two algorithms:

- *MargNet-q*: We replace marginal feature by marginal query in MargNet, denoted as MargNet-q.

- *MargNet-s*: We use a fixed-round iterative marginal selection strategy, which is the same as that in GEM, to select marginals and train them with neural networks.

**6.4.2. Experimental Results.** We present the ablation study results in Table 5. First, marginals are more representative features than marginal queries. As analyzed in Section 3, marginals enable more efficient privacy budget utilization by measuring the frequency distribution over all unique values rather than a single scalar query. This helps MargNet achieve superior synthesis utility compared to MargNet-q.

Second, adaptive selection proves more robust than the fixed-round iterative selection strategy, particularly under a limited privacy budget (e.g.,  $\epsilon = 0.2$ ). We attribute this to the fact that limited privacy budgets necessitate more judicious budget allocation, which adaptive selection provides through its dynamic termination criterion. This advantage persists on the Gauss10 dataset, but the performance gap narrows. Consistent with our findings in Section 6.2, we hypothesize that this is due to the coarse discretization imposed by PrivTree under a limited privacy budget, which introduces substantial discretization errors that overshadow the benefits of adaptive selection.

## 7. Conclusions and Limitations

This work challenges a long-held view that the statistical method, AIM, is universally state-of-the-art in DP tabular data synthesis and proposes a new NN-based approach, MargNet. Through MargNet, we demonstrate that neural networks can achieve superior performance when properly designed, particularly on densely correlated datasets where PGM’s computational constraints limit its effectiveness. Our comprehensive evaluation across sparsely and densely correlated datasets reveals that algorithm effectiveness is highly dataset-dependent: while AIM excels on sparse correlated data, MargNet achieves superior utility on complex, high-dimensional datasets while maintaining significant computational advantages. These findings highlight the importance of selecting suitable synthesis methods based on dataset characteristics rather than relying on a one-size-fits-all solution. We hope this work can open new directions for developing more nuanced DP synthesis algorithms tailored to diverse real-world scenarios.

We acknowledge several limitations of this work. First, as a marginal-based method, MargNet may not be able to capture high-order correlations if they are present in the data. This is because such correlations cannot always be fully represented or reconstructed from the low-dimensional marginals. Second, while our experiments demonstrate MargNet’s advantages on densely correlated datasets, we acknowledge that sparsely correlated datasets may be more prevalent in real-world applications. In such scenarios, AIM remains a strong and efficient solution, and we do not diminish its importance in this field. Our work should be viewed as complementary to AIM, providing an effective alternative for complex cases rather than a universal replacement.

## References

- [1] S. Sangeetha, G. Sudha Sadasivam, and A. Srikanth, "Differentially private model release for healthcare applications," *International Journal of Computers and Applications*, vol. 44, no. 10, pp. 953–958, 2022.
- [2] R. H. Khokhar, B. C. Fung, F. Iqbal, K. Al-Hussaini, and M. Hussain, "Differentially private release of heterogeneous network for managing healthcare data," *ACM Transactions on Knowledge Discovery from Data*, vol. 17, no. 6, pp. 1–30, 2023.
- [3] A. F. Barrientos, A. Bolton, T. Balmat, J. P. Reiter, J. M. de Figueiredo, A. Machanavajjhala, Y. Chen, C. Kneifel, and M. DeLong, "Providing access to confidential research data through synthesis and verification: An application to data on employees of the u.s. federal government," 2018. [Online]. Available: <https://arxiv.org/abs/1705.07872>
- [4] T. Cunningham, G. Cormode, and H. Ferhatosmanoglu, "Privacy-preserving synthetic location data in the real world," in *17th International Symposium on Spatial and Temporal Databases*, ser. SSTD '21. ACM, Aug. 2021, p. 23–33. [Online]. Available: <http://dx.doi.org/10.1145/3469830.3470893>
- [5] R. McKenna, B. Mullins, D. Sheldon, and G. Miklau, "Aim: An adaptive and iterative mechanism for differentially private synthetic data," *arXiv preprint arXiv:2201.12677*, 2022.
- [6] Z. Zhang, T. Wang, N. Li, J. Honorio, M. Backes, S. He, J. Chen, and Y. Zhang, "{PrivSyn}: Differentially private data synthesis," in *30th USENIX Security Symposium (USENIX Security 21)*, 2021, pp. 929–946.
- [7] G. Vietri, C. Archambeau, S. Aydoore, W. Brown, M. Kearns, A. Roth, A. Siva, S. Tang, and S. Z. Wu, "Private synthetic data for multitask learning and marginal queries," *Advances in Neural Information Processing Systems*, vol. 35, pp. 18 282–18 295, 2022.
- [8] T. Liu, J. Tang, G. Vietri, and S. Wu, "Generating private synthetic data with genetic algorithms," in *International Conference on Machine Learning*. PMLR, 2023, pp. 22 009–22 027.
- [9] K. Cai, X. Lei, J. Wei, and X. Xiao, "Data synthesis via differentially private markov random fields," *Proceedings of the VLDB Endowment*, vol. 14, no. 11, pp. 2190–2202, 2021.
- [10] Y. Tao, R. McKenna, M. Hay, A. Machanavajjhala, and G. Miklau, "Benchmarking differentially private synthetic data generation algorithms," 2022. [Online]. Available: <https://arxiv.org/abs/2112.09238>
- [11] K. Chen, X. Li, C. Gong, R. McKenna, and T. Wang, "Benchmarking differentially private tabular data synthesis," 2025. [Online]. Available: <https://arxiv.org/abs/2504.14061>
- [12] T. Liu, G. Vietri, and S. Z. Wu, "Iterative methods for private synthetic data: Unifying framework and new methods," *Advances in Neural Information Processing Systems*, vol. 34, pp. 690–702, 2021.
- [13] F. Harder, K. Adamczewski, and M. Park, "Dp-merf: Differentially private mean embeddings with random features for practical privacy-preserving data generation," in *International conference on artificial intelligence and statistics*. PMLR, 2021, pp. 1819–1827.
- [14] D. Chen, T. Orekondy, and M. Fritz, "Gs-wgan: A gradient-sanitized approach for learning differentially private generators," 2021. [Online]. Available: <https://arxiv.org/abs/2006.08265>
- [15] K. Li, C. Gong, X. Li, Y. Zhao, X. Hou, and T. Wang, "From easy to hard: Building a shortcut for differentially private image synthesis," in *2025 IEEE Symposium on Security and Privacy (SP)*. IEEE, 2025, pp. 3988–4006.
- [16] L. Xie, K. Lin, S. Wang, F. Wang, and J. Zhou, "Differentially private generative adversarial network," *arXiv preprint arXiv:1802.06739*, 2018.
- [17] T. V. Tran and L. Xiong, "Differentially private tabular data synthesis using large language models," *arXiv preprint arXiv:2406.01457*, 2024.
- [18] R. Castellon, A. Gopal, B. Bloniarz, and D. Rosenberg, "Dp-tbart: A transformer-based autoregressive model for differentially private tabular data generation," 2023. [Online]. Available: <https://arxiv.org/abs/2307.10430>
- [19] K. Li, C. Gong, Z. Li, Y. Zhao, X. Hou, and T. Wang, "{PrivImage}: Differentially private synthetic image generation using diffusion models with {Semantic-Aware} pretraining," in *33rd USENIX Security Symposium (USENIX Security 24)*, 2024, pp. 4837–4854.
- [20] C. Gong, K. Li, Z. Lin, and T. Wang, "Dpimagebench: A unified benchmark for differentially private image synthesis," *arXiv preprint arXiv:2503.14681*, 2025.
- [21] J. Jordon, J. Yoon, and M. Van Der Schaar, "Pate-gan: Generating synthetic data with differential privacy guarantees," in *International conference on learning representations*, 2018.
- [22] M. L. Fang, D. S. Dhami, and K. Kersting, "Dp-ctgan: Differentially private medical data generation using ctgans," in *International conference on artificial intelligence in medicine*. Springer, 2022, pp. 178–188.
- [23] M. Bun and T. Steinke, "Concentrated differential privacy: Simplifications, extensions, and lower bounds," 2016. [Online]. Available: <https://arxiv.org/abs/1605.02065>
- [24] C. Dwork, A. Roth *et al.*, "The algorithmic foundations of differential privacy," *Foundations and Trends® in Theoretical Computer Science*, vol. 9, no. 3–4, pp. 211–407, 2014.
- [25] J. Zhang, G. Cormode, C. M. Procopiuc, D. Srivastava, and X. Xiao, "Privbayes: Private data release via bayesian networks," *ACM Transactions on Database Systems (TODS)*, vol. 42, no. 4, pp. 1–41, 2017.
- [26] R. McKenna, D. Sheldon, and G. Miklau, "Graphical-model based estimation and inference for differential privacy," in *International Conference on Machine Learning*. PMLR, 2019, pp. 4435–4444.
- [27] X. Zhang, S. Ji, and T. Wang, "Differentially private releasing via deep generative model (technical report)," *arXiv preprint arXiv:1801.01594*, 2018.
- [28] A. Kotelnikov, D. Baranchuk, I. Rubachev, and A. Babenko, "Tabdpm: Modelling tabular data with diffusion models," in *International Conference on Machine Learning*. PMLR, 2023, pp. 17 564–17 579.
- [29] A. Sablayrolles, Y. Wang, and B. Karrer, "Privately generating tabular data using language models," 2023. [Online]. Available: <https://arxiv.org/abs/2306.04803>
- [30] M. Abadi, A. Chu, I. Goodfellow, H. B. McMahan, I. Mironov, K. Talwar, and L. Zhang, "Deep learning with differential privacy," in *Proceedings of the 2016 ACM SIGSAC Conference on Computer and Communications Security*, ser. CCS'16. ACM, Oct. 2016, p. 308–318. [Online]. Available: <http://dx.doi.org/10.1145/2976749.2978318>
- [31] L. Xu, M. Skoularidou, A. Cuesta-Infante, and K. Veeramachaneni, "Modeling tabular data using conditional gan," 2019. [Online]. Available: <https://arxiv.org/abs/1907.00503>
- [32] R. McKenna, G. Miklau, and D. Sheldon, "Winning the nist contest: A scalable and general approach to differentially private synthetic data," *arXiv preprint arXiv:2108.04978*, 2021.
- [33] R. Rogers, A. Roth, J. Ullman, and S. Vadhan, "Privacy odometers and filters: Pay-as-you-go composition," 2021. [Online]. Available: <https://arxiv.org/abs/1605.08294>
- [34] M. Cesar and R. Rogers, "Bounding, concentrating, and truncating: Unifying privacy loss composition for data analytics," 2020. [Online]. Available: <https://arxiv.org/abs/2004.07223>
- [35] V. Feldman and T. Zrnic, "Individual privacy accounting via a renyi filter," 2022. [Online]. Available: <https://arxiv.org/abs/2008.11193>
- [36] M. Fuentes, B. Mullins, R. McKenna, G. Miklau, and D. Sheldon, "Joint selection: Adaptively incorporating public information for private synthetic data," 2024. [Online]. Available: <https://arxiv.org/abs/2403.07797>

- [37] G. Vietri, G. Tian, M. Bun, T. Steinke, and Z. S. Wu, “New oracle-efficient algorithms for private synthetic data release,” 2020. [Online]. Available: <https://arxiv.org/abs/2007.05453>
- [38] “Adult dataset,” 2016. [Online]. Available: <https://www.kaggle.com/datasets/wenrui/adult-income-dataset>
- [39] S. Moro, P. Rita, and P. Cortez, “Bank Marketing,” UCI Machine Learning Repository, 2014, DOI: <https://doi.org/10.24432/C5K306>.
- [40] “Loan dataset,” 2020. [Online]. Available: <https://www.kaggle.com/datasets/devanshi23/loan-data-2007-2014>
- [41] Y. Du and N. Li, “Towards principled assessment of tabular data synthesis algorithms,” *arXiv preprint arXiv:2402.06806*, 2024.
- [42] J. Zhang, X. Xiao, and X. Xie, “Privtree: A differentially private algorithm for hierarchical decompositions,” in *Proceedings of the 2016 international conference on management of data*, 2016, pp. 155–170.
- [43] C. Eckart and G. Young, “The approximation of one matrix by another of lower rank,” *Psychometrika*, vol. 1, no. 3, pp. 211–218, 1936.
- [44] E. Hoogetboom, D. Nielsen, P. Jaini, P. Forré, and M. Welling, “Argmax flows and multinomial diffusion: Learning categorical distributions,” 2021. [Online]. Available: <https://arxiv.org/abs/2102.05379>

## Appendix A. Data Preprocessing

Aligning with previous works [5], [6], [10], [11], we also need to utilize some preprocessing methods to make sure all methods can work across different datasets.

- **PrivTree Discretization.** PrivTree algorithm [42] can divide a continuous value range under differential privacy. Here, we apply PrivTree to AIM, MargNet, GEM, PrivSyn, and RAP++ in Gaussian datasets.
- **Rare Category Filtering.** We follow the filtering method for categorical attributes proposed by Chen et al. [11], which introduces both a  $3\sigma$  criterion [6], [32] and a fixed filter threshold, guaranteeing the simplicity of the dataset.

## Appendix B. Detailed Proof

### B.1. Proof of Theorem 3

First, we present a result from Eckart and Young [43].

**Lemma 1.** Let  $\lambda_1, \dots, \lambda_r$  be the singular values of  $P$ , sorted in descending order. Then the minimum approximation error when approximating  $P$  by a rank- $m$  matrix is

$$\min_{\text{rank}(Q) \leq m} \|P - Q\|_F^2 = \sum_{t=m+1}^r \lambda_t^2.$$

For a batch of samples, we use the average of the distribution of each row as the final marginal estimation. Therefore, the error  $\mathcal{L}(G)$  can be written as

$$\mathcal{L}_s(G) = \sum_{i \in I_s} \left\| M_i - \frac{\hat{N}}{b} \sum_{j=1}^b u_j^T v_j \right\|_F^2,$$

where  $u_j$  and  $v_j$  are the one-way marginals of two attributes in the  $j$ -th sample row. (If  $M_i$  itself is a one-way marginal, we can simply set  $v_j$  to be a  $1 \times 1$  matrix.) Note that the rank of  $\sum_{j=1}^b u_j^T v_j$  is at most  $b$  since it is a sum of  $b$  rank-one matrices. By Lemma 1, we have

$$\mathcal{L}_s(G) = \sum_{i \in I_s} \left\| \frac{1}{b} \sum_{j=1}^b u_j^T v_j - M_i \right\|_F^2 \geq \sum_{i \in I_s} \left( \sum_{t=b+1}^{r(M_i)} \lambda_t^2 \right),$$

which is a consequence of Theorem 3.

### B.2. Proof of Theorem 4

We first decompose  $\mathcal{L}_s(G)$  into two terms. By the inequality  $\|A + B\|_F^2 \leq 2(\|A\|_F^2 + \|B\|_F^2)$ , we have

$$\begin{aligned} \mathcal{L}_s(G) &= \sum_{i \in I_s} \left\| M_i - \bar{M}_i + \bar{M}_i - \hat{M}_i(G) \right\|_F^2 \\ &\leq 2 \sum_{i \in I_s} \left( \left\| \bar{M}_i - \hat{M}_i(G) \right\|_F^2 + \left\| M_i - \bar{M}_i \right\|_F^2 \right). \end{aligned} \quad (12)$$

Note that  $\|\bar{M}_i - \hat{M}_i(G)\|_F^2$  is computable from our model, so it suffices to bound  $\|M_i - \bar{M}_i\|_F^2$ . Recall that  $\bar{M}_i = M_i + \mathcal{N}(0, \bar{\sigma}_i^2 \mathbb{I})$ , which implies

$$M_i - \bar{M}_i \sim \mathcal{N}(0, \bar{\sigma}_i^2)^{n_i}.$$

Consequently,

$$\|M_i - \bar{M}_i\|_F^2 \sim \bar{\sigma}_i^2 \chi_{n_i}^2,$$

where  $\chi_{n_i}^2$  denotes the chi-squared distribution with  $n_i$  degrees of freedom. Let  $F_{\chi_{n_i}^2}^{-1}$  denote the inverse cumulative distribution function of  $\chi_{n_i}^2$ . Then for any  $\delta_i \in (0, 1)$ , with probability at least  $1 - \delta_i$ ,

$$\|M_i - \bar{M}_i\|_F^2 \leq \bar{\sigma}_i^2 F_{\chi_{n_i}^2}^{-1}(1 - \delta_i).$$

Applying this bound to Equation (12) yields Theorem 4.

### B.3. Proof of Theorem 5

To prove Theorem 5, we first give a primary conclusion [24].

**Lemma 2.** Assuming the final selected marginal during the adaptive framework is  $M_K$ , then with at least probability  $1 - \delta$ , the following inequality holds for any  $i \neq K$ .

$$q(i) \leq q(K) + \frac{\Delta q}{\sqrt{2\rho_s^k}} \log(|C|/\delta), \quad (13)$$

where  $C$  is the candidate set,  $q_i$  is defined in Algorithm 2.

For the final model  $G$ , we can build the error estimation with the model before the last selection step  $G^{K-1}$ . Assuming that we have conducted  $K$  selection steps and marginal  $M_i$  is not selected, and the marginal fitted by the

TABLE 6: Results of DP-MERF and DP-TabDDPM on sparsely correlated datasets.

Dataset	Method	ML Efficacy						Query Error						Fidelity Error					
		0.2	0.5	1.0	2.0	5.0	10.0	0.2	0.5	1.0	2.0	5.0	10.0	0.2	0.5	1.0	2.0	5.0	10.0
Adult	DP-MERF	0.63	0.73	0.71	0.72	0.72	0.72	0.019	0.018	0.018	0.018	0.017	0.016	0.324	0.296	0.265	0.266	0.218	0.267
	DP-TabDDPM	0.43	0.43	0.43	0.43	0.43	0.43	0.075	0.045	0.039	0.038	0.039	0.038	0.889	0.443	0.378	0.341	0.328	0.321
Bank	DP-MERF	0.61	0.61	0.63	0.62	0.61	0.61	0.012	0.011	0.008	0.009	0.009	0.010	0.332	0.312	0.274	0.280	0.280	0.299
	DP-TabDDPM	0.47	0.47	0.47	0.47	0.47	0.47	0.105	0.092	0.070	0.068	0.057	0.053	0.474	0.649	0.754	0.761	0.715	0.703
Loan	DP-MERF	0.22	0.18	0.24	0.21	0.21	0.18	0.058	0.063	0.063	0.060	0.060	0.059	0.902	0.894	0.887	0.904	0.922	0.904
	DP-TabDDPM	0.24	0.24	0.24	0.25	0.26	0.25	0.059	0.055	0.059	0.055	0.054	0.056	0.901	0.896	0.891	0.885	0.873	0.874

TABLE 7: Hyperparameters of MargNet.  $T$  and  $T^*$  are training iterations under  $0.2 \leq \varepsilon \leq 5.0$  and  $\varepsilon = 10.0$ , respectively. Here  $G$  is the abbreviation of Gauss.

	Adult	Bank	Loan	G10	G30	G50
Training Iter. $T$	200	200	1000	200	200	500
Training Iter. $T^*$	100	100	1000	100	100	500
Learning Rate $r$	0.001	0.001	0.001	0.001	0.001	0.001
Batch Size $b$	512	512	512	256	1024	1024
Parameter $c$	16d	16d	16d	16d	16d	16d
$r_i$	1.0	1.0	1.0	1.0	1.0	1.0

model  $G$  and intermediate model  $G^{K-1}$  are  $\hat{M}_i$  and  $\hat{M}_i^{K-1}$ , respectively, we have

$$\left\| M_i - \hat{M}_i \right\|_1 \leq \left\| M_i - \hat{M}_i^{K-1} \right\|_1 + \left\| \hat{M}_i^{K-1} - \hat{M}_i \right\|_1 \quad (14)$$

Here, we bound the fitting error of the unselected marginal by two terms: one is the fitting error in the last selection round, and the other one the improvement from the model fitting after the last selection round.

Then, by Lemma 2, we have that with probability  $1 - \delta$ ,

$$\begin{aligned} r_i \left( \left\| M_i - \hat{M}_i^{K-1} \right\|_1 - n_i / \sqrt{\pi \rho_K^S} \right) \\ \leq r_\theta \left( \left\| M_\theta - \hat{M}_\theta^{K-1} \right\|_1 - n_\theta / \sqrt{\pi \rho_K^S} \right) + \frac{\Delta_q}{\sqrt{2\rho_s^k}} \log \frac{|C|}{\delta} \end{aligned}$$

Rearranging the above inequality, we obtain that for any unselected marginal  $M_i$  and the finally selected marginal  $M_\theta$ ,

$$\begin{aligned} \left\| M_i - \hat{M}_i^{K-1} \right\|_1 &\leq \frac{r_\theta}{r_i} \left\| M_\theta - \hat{M}_\theta^{K-1} \right\|_1 \\ &+ \frac{n_i r_i - n_\theta r_\theta}{r_i \sqrt{\pi \rho_s^K}} + \frac{\Delta_q}{r_i \sqrt{2\rho_s^K}} \log \frac{|C|}{\delta} \end{aligned} \quad (15)$$

holds with at least probability  $1 - \delta$ .  $r_i$  and  $r_\theta$  are the weights used in exponential mechanism in Algorithm 2, and  $\rho_s^K$  is the value of  $\rho_s$  in the last selection iteration.

We denote the RHS of Equation (10) as  $B_{i,K}$ . Then by Equation (14), we can obtain an upper bound of the total  $\ell_1$  error of unselected marginals. Then with Equation (14), we have

$$\sum_i \left\| M_i - \hat{M}_i \right\|_1 \leq \sum_i B_{i,K} + \sum_i \left\| \hat{M}_i^{K-1} - \hat{M}_i \right\|_1,$$

as claimed in Theorem 5.

TABLE 8: Comparison of MargNet (with 10-uniform binning) with DP-CTGAN and DP-MERF under  $\varepsilon = 0.2$ .

Metric	Dataset	MargNet	DP-CTGAN	DP-MERF
Query Err.	Gauss10	<b>0.025</b>	0.055	0.223
	Gauss30	<b>0.017</b>	0.058	0.217
	Gauss50	<b>0.017</b>	0.035	0.018
Fidelity Err.	Gauss10	<b>0.35</b>	0.58	0.99
	Gauss30	<b>0.26</b>	0.57	0.96
	Gauss50	<b>0.25</b>	0.45	0.27

## Appendix C. Implementation Details

As introduced earlier, MargNet involves multiple training hyperparameters. We provide the relevant implementation details. The hyperparameter settings are summarized in Table 7. Some extra details are provided as follows.

- **Network Architecture.** We adopt the same network structure as in prior work [12], [22]. The detailed architecture is available in our open-source repository and is omitted here for brevity.
- **Parameter  $c$ .** Following AIM, we set  $c = 16d$  for all datasets, where  $d$  is the dimension of the dataset. This constraint ensures that at most  $16d$  marginals are selected during Algorithm 2, which also motivates our choice of  $d$  as the weight enhancement factor for newly selected marginals.
- **Training Iterations.** We present the setting of training iteration, learning rate and batch size in Table 7. Notably, **we use fewer training iterations for larger privacy budgets**  $\varepsilon$  on most datasets. This counterintuitive choice is motivated by the fact that larger  $\varepsilon$  allows selecting more marginals, which in turn increases the effective number of training iterations in our model. Reducing the nominal iteration count in these cases provides two benefits: (1) it prevents overfitting and yields more stable results, and (2) it accelerates model fitting without significantly compromising utility.

## Appendix D. Supplementary Experimental Results

### D.1. Supplementary Results of Baselines

In Appendix 6.1 and Appendix 6.2, we discussed DP-TabDDPM and DP-MERF but do not present their ex-

TABLE 9: Results of DP-MERF and DP-TabDDPM on densely correlated datasets.

Dataset	Method	Query Error						Fidelity Error						Running Time (min)					
		0.2	0.5	1.0	2.0	5.0	10.0	0.2	0.5	1.0	2.0	5.0	10.0	0.2	0.5	1.0	2.0	5.0	10.0
Gauss10	DP-MERF	0.223	0.037	0.192	0.027	0.028	0.027	0.985	0.475	0.966	0.456	0.478	0.420	0.06	0.06	0.20	0.06	0.16	0.06
	DP-TabDDPM	0.216	0.195	0.201	0.196	0.200	0.194	0.906	0.855	0.877	0.835	0.879	0.862	0.87	0.67	0.76	0.76	0.76	0.76
Gauss30	DP-MERF	0.217	0.225	0.209	0.233	0.049	0.049	0.963	0.969	0.947	0.956	0.347	0.392	0.12	0.16	0.12	0.12	0.12	0.12
	DP-TabDDPM	0.234	0.213	0.199	0.207	0.202	0.196	0.955	0.907	0.879	0.893	0.880	0.865	8.95	8.77	9.08	8.83	8.68	8.86
Gauss50	DP-MERF	0.018	0.016	0.018	0.032	0.019	0.035	0.274	0.297	0.335	0.307	0.287	0.338	0.20	0.17	0.22	0.18	0.17	0.17
	DP-TabDDPM	0.239	0.251	0.242	0.248	0.245	0.249	0.959	0.983	0.965	0.979	0.972	0.978	23.09	22.54	22.39	16.59	15.54	15.52

TABLE 10: Ablation study results on Adult dataset. We investigate three hyperparameters under  $\epsilon = 1.0$ . Bold values are the default values in previous experiments.

	Value	ML Eff.	Query Err.	Fidelity Err.
Learning Rate	1e-2	0.768	0.0122	0.0224
	<b>1e-3</b>	0.763	0.0117	0.0217
	1e-4	0.768	0.0112	0.0203
	1e-5	0.747	0.0119	0.0298
Training Iterations	50	0.762	0.0125	0.0209
	<b>100</b>	0.763	0.0117	0.0217
	200	0.764	0.0114	0.0219
	400	0.767	0.0129	0.0232
Batch Size	32	0.725	0.0127	0.0423
	128	0.745	0.0129	0.0276
	<b>512</b>	0.763	0.0117	0.0217
	1024	0.768	0.0119	0.0218

perimental results. These methods’ performance is inferior to that of other methods. We now present these results here. For DP-TabDDPM and DP-MERF’s results on real-world datasets, we present them in Table 6. The densely correlated dataset results are provided in Table 9.

On Gauss50 dataset, DP-MERF exhibits results similar to those of DP-CTGAN, achieving strong performance at very low values of  $\epsilon$  on densely correlated datasets. We previously attributed this to the coarse discretization used by marginal-based methods rather than to the strong synthesis ability of DP-MERF or DP-CTGAN. To support this explanation, we present MargNet’s performance on densely correlated datasets under 10-uniform binning (bin number = 10) in Table 8. We can easily observe that under uniform binning, MargNet achieves higher utility than DP-MERF and DP-CTGAN. In the experiments described in the main text, we select PrivTree because it adaptively partitions domains according to the privacy budget, resulting in more precise discretization when the budget is sufficient.

## D.2. Ablation Study of Training Hyperparameters

In this subsection, we conduct some ablation experiments on training parameters (learning rate, training iterations, and batch size). For simplicity, we conduct experiments on  $\epsilon = 10.0$  and on Adult dataset, as shown in Table 10. For the learning rate, when it decreases to a low level (e.g., 1e-5), we observe a slight drop in performance. We believe this occurs because the model cannot converge under such a small learning rate. For training iteration, we

TABLE 11: Maximum memory cost of different algorithms. NN (all) and PGM (all) mean utilizing the neural network and PGM to fit all pairwise marginals, respectively. The results are obtained on Adult dataset.

$\epsilon$	MargNet	NN (all)	AIM	PGM (all)
1.0	68 MB	206 MB	597 MB	> 1 TB
10.0	130 MB	206 MB	1.55 GB	> 1 TB

find that within a reasonable interval, it does not significantly influence the model performance. A notable hyperparameter is batch size, which in our analysis can affect the model’s theoretical fitting ability. In the ablation study, when the batch size is small (e.g.,  $b = 32$ ), the performance degrades.

## D.3. Memory Comparison of AIM and MargNet

Another key factor we consider when selecting algorithms to generate data. This subsection will provide the memory cost of PGM and neural networks. We mainly consider three cases: NN with all marginals, NN in MargNet, PGM with all marginals, and PGM in AIM. Notice that AIM is a CPU algorithm, but neural networks require GPUs. We only count the peak memory cost on the respective devices. The results are provided in Table 11.

Firstly, aligning with what we mentioned, when we require fitting all pairwise marginals, PGM consumes much memory (> 1 TB). The phenomenon is caused by the extremely large clique, whose domain size is equal to that of the whole dataset. In contrast, even with all marginals, neural networks can still work with relatively lower memory costs (206 MB). Furthermore, although we separate the marginal case and directly compare MargNet and AIM, the PGM still requires more memory than MargNet. Finally, we also need to clarify that these results are only on Adult dataset. When dealing with other large datasets with plenty of privacy budget, MargNet is likely to cost more memory. This is because AIM constraints the marginal candidates to control the model size and make optimization feasible, but MargNet does not set any limitation.

## D.4. Fixing Input

When representing the dataset by features (e.g., marginals), our objective becomes producing a batch of outputs that preserve these features more effectively. Accordingly, if the features are fixed, increased output diversity does not contribute to achieving this objective. In

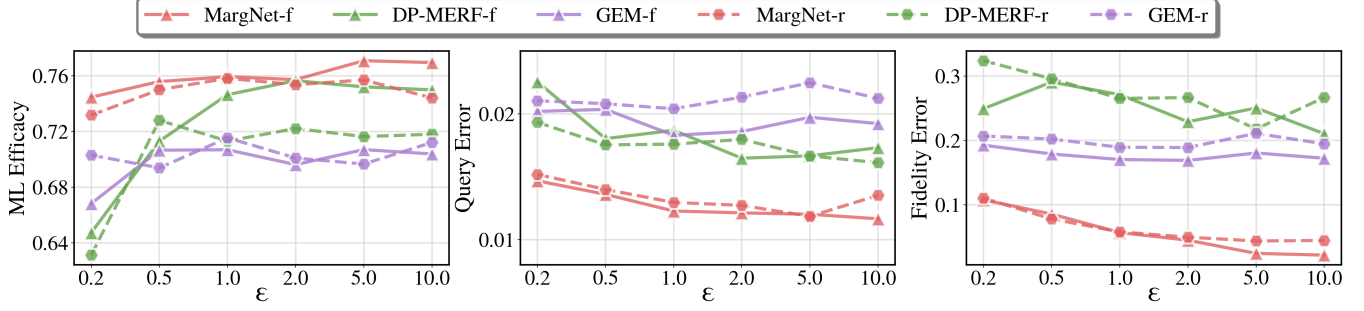
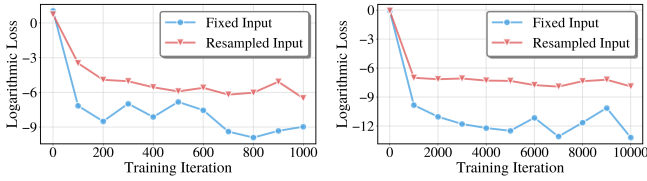


Figure 8: Machine learning efficacy, query errors, and fidelity errors of MargNet, DP-MERF, GEM on Adult dataset. The real lines (“-f”) mean methods with fixed input, and the dashed lines (“-r”) mean methods with resampled input.



(a) Random Fourier feature (b) Marginal feature

Figure 9: Training loss under fixed and resampled input.

this case, we hypothesize that using a fixed model input (e.g., sampling input once at initialization and fixing it as the input for any future model access) can be helpful in model training on feature-based models. In this section, we conduct experiments on whether fixing input noise can have a positive influence on those feature-DP methods:

- We pre-compute random Fourier feature (used in DP-MERF) and marginals (used in MargNet and a special case in GEM), and train the neural network on these features. The loss tracks are plotted in Figure 9a and Figure 9b, respectively.
- We directly compare the utility performances of MargNet, GEM, and DP-MERF with those of these algorithms with fixed input. The results are illustrated in Figure 8.

In Figure 9, a straightforward observation is that with fixed input, NN’s training loss can converge to a lower level in limited training iterations. We believe this is because fixed input reduces the complexity of the map from input to output and helps models learn better. In Figure 8, the performances of MargNet, DP-MERF, and GEM under fixed input are not necessarily inferior to their counterparts under resampled input; in fact, they are sometimes superior. These results lend support to our conjecture that fixing the input has at least no detrimental effect on the model’s training or final generative performance. Therefore, in our main experiments, we uniformly adopt this fixed-input setting for MargNet.

## Appendix E. Scalability to Other Models

In our experiments, the network architecture we consider is primarily an MLP, which is commonly used as a data gen-

---

### Algorithm 4: Marginal Training (Diffusion)

---

**Input:** Model  $G$  parameterized by  $\theta$ , iteration  $T$ , learning rate  $r$ , a set of marginals  $S$ , Hyperparameter  $w_{1:|S|}$ , timesteps  $T_s$ .

**Output:** Model after training  $G$ .

```

1  $t = 0$ ;
2 while  $t < T$  do
3    $G_t = G$ ;
4   for  $s = T_s, \dots, 1$  do
5     Generate  $D'_{s+1}$  by denoising  $G_t$ ;
6     Obtain  $D'_s = \text{denoise\_fn}(D'_{s+1})$ ;
7     Compute loss:
           
$$\tilde{M}_i(s) = \bar{\alpha}_s \tilde{M}_i + (1 - \bar{\alpha}_s) \frac{1}{n_i}$$

           
$$\mathcal{L}(\theta, S) = \sum_{i=1}^{|S|} w_i \left\| M_i(D'_s) - \tilde{M}_i(s) \right\|_2^2$$

8     Update model  $\theta = \theta - r \nabla_{\theta} \mathcal{L}(\theta, S)$ ;
9    $t = t + 1$ ;
10 return  $G$ .
```

---

erator in GANs. However, the “marginal + neural network” pattern is a general concept. We believe its potential extends beyond MLPs and could be applied to other advanced generative architectures, such as diffusion models or LLMs. As a preliminary exploration of this idea, we briefly propose a conceptual framework here, as shown in Algorithm 4.

Algorithm 4 draws on the Multinomial Diffusion model from Hooeboom et al.’s work [44]. In their work, they consider the diffusion process of categorical variables, which can be formulated as:

$$q(x_t | x_{t-1}) = \mathcal{C}(x_t | \alpha_t x_{t-1} + (1 - \alpha_t) \frac{1}{n})$$

Here  $n$  is the total number of categories. It implies that the generation process starts from a uniform distribution. In this case, we can calculate the marginal on those “intermediate” samples  $x_t$ . Then we can obtain the marginal error to build a loss function in each diffusion timestep and train the model.